28. F. Aharonian *et al.*, *Astron. Astrophys.* **499**, 273 (2009).
29. A. A. Abdo *et al.*, *Astrophys. J. Suppl. Ser.* **183**, 46 (2009).
30. B. J. McLean, G. R. Greene, M. G. Lattanzi, B. Pirenne, *ASP Conf. Ser.* **216**, 145 (2000).
31. The Fermi LAT Collaboration is supported by NASA and the U.S. Department of Energy; the Commissariat à l'Énergie Atomique and CNRS/Institut National de Physique Nucleaire et de Physique des Particules (France); the Agenzia Spaziale Italiana and Istituto Nazionale di Fisica Nucleare (Italy); the Ministry of Education, Culture, Sports, Science and Technology, High Energy Accelerator Research Organization (KEK), and Japan Aerospace Exploration Agency (Japan); and the K. A. Wallenberg Foundation, Swedish Research Council, and National Space Board (Sweden). Additional support was provided by the Istituto Nazionale di Astrofisica (Italy) and the Centre National d'Études Spatiales (France).

Supporting Online Material
www.sciencemag.org/cgi/content/full/325/5942/845/DC1
SOM Text
Figs. S1 and S2
References

29 May 2009; accepted 20 July 2009
10.1126/science.1177023

A Population of Gamma-Ray Millisecond Pulsars Seen with the Fermi Large Area Telescope

A. A. Abdo,[1]* M. Ackermann,[2] M. Ajello,[2] W. B. Atwood,[3] M. Axelsson,[4,5] L. Baldini,[6] J. Ballet,[7] G. Barbiellini,[8,9] M. G. Baring,[10] D. Bastieri,[11,12] B. M. Baughman,[13] K. Bechtol,[2] R. Bellazzini,[6] B. Berenji,[2] G. F. Bignami,[14] R. D. Blandford,[2] E. D. Bloom,[2] E. Bonamente,[15,16] A. W. Borgland,[2] J. Bregeon,[6] A. Brez,[6] M. Brigida,[17,18] P. Bruel,[19] T. H. Burnett,[20] G. A. Caliandro,[17,18] R. A. Cameron,[2] F. Camilo,[21] P. A. Caraveo,[22] P. Carlson,[4,23] J. M. Casandjian,[7] C. Cecchi,[15,16] Ö. Çelik,[24] E. Charles,[2] A. Chekhtman,[1,25] C. C. Cheung,[24] J. Chiang,[2] S. Ciprini,[15,16] R. Claus,[2] I. Cognard,[26] J. Cohen-Tanugi,[27] L. R. Cominsky,[28] J. Conrad,[4,23,29]† R. Corbet,[24,30] S. Cutini,[31] C. D. Dermer,[1] G. Desvignes,[26] A. de Angelis,[32] A. de Luca,[14] F. de Palma,[17,18] S. W. Digel,[2] M. Dormody,[3] E. do Couto e Silva,[2] P. S. Drell,[2] R. Dubois,[2] D. Dumora,[33,34] Y. Edmonds,[2] C. Farnier,[27] C. Favuzzi,[17,18] S. J. Fegan,[19] W. B. Focke,[2] M. Frailis,[32] P. C. C. Freire,[35] Y. Fukazawa,[36] S. Funk,[2] P. Fusco,[17,18] F. Gargano,[18] D. Gasparrini,[31] N. Gehrels,[24,37] S. Germani,[15,16] B. Giebels,[19] N. Giglietto,[17,18] F. Giordano,[17,18] T. Glanzman,[2] G. Godfrey,[2] I. A. Grenier,[7] M. H. Grondin,[33,34] J. E. Grove,[1] L. Guillemot,[33,34]‡ S. Guiriec,[38] Y. Hanabata,[36] A. K. Harding,[24] M. Hayashida,[2] E. Hays,[24] G. Hobbs,[39] R. E. Hughes,[13] G. Jóhannesson,[2] A. S. Johnson,[2] R. P. Johnson,[3] T. J. Johnson,[24,37]‡ W. N. Johnson,[1] S. Johnston,[39] T. Kamae,[2] H. Katagiri,[36] J. Kataoka,[40] N. Kawai,[41,42] M. Kerr,[20]‡ J. Knödlseder,[43] M. L. Kocian,[2] M. Kramer,[44] M. Kuss,[6] J. Lande,[2] L. Latronico,[6] M. Lemoine-Goumard,[33,34] F. Longo,[8,9] F. Loparco,[17,18] B. Lott,[33,34] M. N. Lovellette,[1] P. Lubrano,[15,16] G. M. Madejski,[2] A. Makeev,[1,25] R. N. Manchester,[39] M. Marelli,[22] M. N. Mazziotta,[18] W. McConville,[24,37] J. E. McEnery,[24] M. A. McLaughlin,[45] C. Meurer,[4,29] P. F. Michelson,[2] W. Mitthumsiri,[2] T. Mizuno,[36] A. A. Moiseev,[37,46] C. Monte,[17,18] M. E. Monzani,[2] A. Morselli,[47] I. V. Moskalenko,[2] S. Murgia,[2] P. L. Nolan,[2] J. P. Norris,[48] E. Nuss,[27] T. Ohsugi,[36] N. Omodei,[6] E. Orlando,[49] J. F. Ormes,[48] D. Paneque,[2] J. H. Panetta,[2] D. Parent,[33,34] V. Pelassa,[27] M. Pepe,[15,16] M. Pesce-Rollins,[6] F. Piron,[27] T. A. Porter,[3] S. Rainò,[17,18] R. Rando,[11,12] S. M. Ransom,[50] P. S. Ray,[1] M. Razzano,[6] N. Rea,[51,52] A. Reimer,[2,53] O. Reimer,[2,53] T. Reposeur,[33,34] S. Ritz,[24] L. S. Rochester,[2] A. Y. Rodriguez,[52] R. W. Romani,[2] M. Roth,[20] F. Ryde,[4,23] H. F. W. Sadrozinski,[3] D. Sanchez,[19] A. Sander,[13] P. M. Saz Parkinson,[3] J. D. Scargle,[54] T. L. Schalk,[3] C. Sgrò,[6] E. J. Siskind,[55] D. A. Smith,[33,34]‡ P. D. Smith,[13] G. Spandre,[6] P. Spinelli,[17,18] B. W. Stappers,[44] J. L. Starck,[7] E. Striani,[47,56] M. S. Strickman,[1] D. J. Suson,[57] H. Tajima,[2] H. Takahashi,[36] T. Tanaka,[2] J. B. Thayer,[2] J. G. Thayer,[2] G. Theureau,[26] D. J. Thompson,[24] S. E. Thorsett,[3] L. Tibaldo,[11,12] D. F. Torres,[52,58] G. Tosti,[15,16] A. Tramacere,[2,59] Y. Uchiyama,[2] T. L. Usher,[2] A. Van Etten,[2] V. Vasileiou,[30,46] C. Venter,[24,60] N. Vilchez,[43] V. Vitale,[47,56] A. P. Waite,[2] E. Wallace,[20] P. Wang,[2] K. Watters,[2] N. Webb,[43] P. Weltevrede,[39] B. L. Winer,[13] K. S. Wood,[1] T. Ylinen,[4,23,61] M. Ziegler[3]

Pulsars are born with subsecond spin periods and slow by electromagnetic braking for several tens of millions of years, when detectable radiation ceases. A second life can occur for neutron stars in binary systems. They can acquire mass and angular momentum from their companions, to be spun up to millisecond periods and begin radiating again. We searched Fermi Large Area Telescope data for pulsations from all known millisecond pulsars (MSPs) outside of globular clusters, using rotation parameters from radio telescopes. Strong gamma-ray pulsations were detected for eight MSPs. The gamma-ray pulse profiles and spectral properties resemble those of young gamma-ray pulsars. The basic emission mechanism seems to be the same for MSPs and young pulsars, with the emission originating in regions far from the neutron star surface.

After the discovery of pulsars, 15 years elapsed before instrumental and computing advances enabled the first radio detections of neutron stars with millisecond spin periods (*1*). Similarly, 17 years after the launch of the Compton Gamma Ray Observatory (CGRO), the Large Area Telescope (LAT) on the Fermi Gamma-ray Space Telescope (formerly GLAST) is now revealing new classes of GeV gamma-ray pulsars. Here, we report LAT detections of pulsed gamma rays from eight galactic millisecond pulsars (MSPs), confirming the marginal detection of PSR J0218+4232 made using the Energetic Gamma Ray Experiment Telescope (EGRET) detector on CGRO (*2*), and including the first MSP seen with the LAT, PSR J0030+0451 (*3*). A companion article (*4*) describes the discovery of 16 young pulsars on the basis of their gamma-ray emission alone. In addition, the LAT has detected about 20 young, radio-loud pulsars (*5*–*7*). The AGILE collaboration has recently detected pulsed gamma-ray emission from an MSP in the globular cluster M28 (*8*).

The Fermi LAT measurements of pulsars in all three of these categories will clarify how neutron stars accelerate the charged particles that radiate at gamma-ray and lower energies. Observed pulse profiles depend on the beam shapes and how they sweep across Earth; comparison of the radio, x-ray, and gamma-ray profiles constrains models of beam formation in pulsar magnetospheres. For gamma-ray pulsars, the high-energy emission dominates the power of the observed electromagnetic radiation (*9*). Consequently, gamma rays provide a probe of these cosmic accelerators. Millisecond pulsars shine for billions of years longer than do normal pulsars. We now know that they can radiate brightly in gamma rays.

The LAT images the entire sky every 3 hours at photon energies from 20 MeV to >300 GeV (*10*). Incident gamma rays convert to electron-positron pairs in tungsten foils, leaving tracks in single-sided silicon strip detectors that provide the photon direction. A hodoscopic CsI calorimeter samples the photon energy, and charged particles are rejected through the use of information from a segmented scintillator array.

MSPs form a distinct class, with small spin periods ($P < 30$ ms) and minuscule braking rates ($\dot{P} < 10^{-17}$). Most are in binary systems. The idea that they have been spun up by the torque resulting from accretion of mass from their companions (*11*) is supported by the recent observations reported in (*12*). MSPs are 10^8 to 10^{10} years old, whereas the young gamma-ray pulsars are 10^3 to 10^5 years old. Their surface magnetic fields are a factor of 10^4 weaker than when the neutron star first formed. However, both the rate of rotational kinetic energy loss, $\dot{E} = 4\pi^2 I\dot{P}/P^3$ (on the assumptions of dipole magnetic fields and a neutron star moment of inertia $I = 10^{45}$ g·cm²), and the magnetic field at the light cylinder, $B_{LC} = 4\pi^2(3I\dot{P}/2c^3P^5)^{1/2}$ (where c is the speed of light), are comparable to those of newly formed pulsars (*13*). On the basis of theoretical models of gamma-ray emission from MSPs, it

was predicted that Fermi would detect roughly 10 pulsed detections in 1 year (*14*, *15*).

The Australia Telescope National Facility (ATNF) pulsar database, V1.35 (*16*, *17*), lists 1794 spin-powered pulsars, of which 168 have $P < 30$ ms and $\dot{P} < 10^{-17}$. Of these, 96 are in globular clusters (*18*). Here, we consider the 72 remaining field MSPs. A radio and x-ray pulsar timing campaign provided rotation ephemerides for Fermi (*19*). MSP timing solutions were obtained from the Nançay Radio Telescope (*20*), the Parkes Radio Telescope (*21*), the Green Bank Telescope (*22*), the Lovell Telescope at Jodrell Bank Observatory (*23*), the Arecibo Observatory radio telescope (*24*), and the Westerbork Synthesis Radio Telescope (*25*). For six of the field MSPs, we used noncontemporaneous ephemerides from the ATNF database. The timing parameters used in this work will be made available on the servers of the Fermi Science Support Center (*26*).

For the gamma-ray timing analysis, we used LAT data acquired from 30 June 2008 to 15 March 2009, selecting events with energy > 0.1 GeV that passed the diffuse gamma-ray selection cuts (*10*). For pulsars with galactic latitude $|b| > 10°$, we selected events within 1° of the radio position; this threshold was reduced to 0.5° for $|b| < 10°$ because of the bright gamma-ray background in the galactic plane resulting from cosmic rays interacting with the interstellar medium. LAT photon arrival times were recorded with an accuracy relative to UTC better than 1 μs (*27*).

Following this analysis, eight MSPs showed strong gamma-ray pulsations with H-test (*28*) values of >25 (Fig. 1 and Table 1). Three are associated with EGRET sources: PSRs J0030+0451, J0218+4232, and J1614–2230. The latter was discovered in a radio search of unidentified EGRET sources (*29*). All of the detected pulsars had con-

Table 1. Properties of the millisecond pulsars detected by Fermi. For each pulsar we give the galactic longitude and latitude (l, b), the rotational period P, the distance d, and the spin-down power $\dot{E}$. Pulsars marked "b" belong to binary systems. The distances come from parallax measurements except for the values marked by an asterisk, which are based on the dispersion measure. The $\dot{E}$ values have been computed using period derivatives corrected for the Shklovskii effect (*36*). The δ parameter gives the phase offset between the maximum of the radio emission and that of the nearest gamma-ray peak, and Δ is the peak separation for two-peaked gamma-ray profiles. Integral photon and energy fluxes over 0.1 GeV are given, as well as spectral indices, exponential cutoff energies, and gamma-ray emission efficiencies η. The systematic uncertainties stemming from the instrument response and the diffuse background are (–0.1, +0.3) for Γ, (–10%, +20%) for E_c, (–10%, +30%) for the photon flux, and (–10%, +20%) for the energy flux.

Pulsar name	l, b	P (ms)	d (pc)	Log $\dot{E}$ (ergs s^{-1})	δ	Δ	Photon flux >0.1 GeV (10^{-8} photons cm^{-2} s^{-1})	Energy flux >0.1 GeV (10^{-11} ergs cm^{-2} s^{-1})	Spectral index	Exponential cutoff energy (GeV)	η (%)
J0030+0451	113.1°, –57.6°	4.865	300 ± 90	33.54	0.16	0.45	5.5 ± 0.7	4.9 ± 0.3	1.3 ± 0.2	1.9 ± 0.4	15 ± 9
J0218+4232 (b)	139.5°, –17.5°	2.323	2700 ± 600*	35.39	0.50	—	5.6 ± 1.3	3.5 ± 0.5	2.0 ± 0.2	7 ± 4	13 ± 6
J0437–4715 (b)	253.4°, –42.0°	5.757	156 ± 2	33.46	0.45	—	4.4 ± 1.0	1.9 ± 0.3	2.1 ± 0.3	2.1 ± 1.1	1.9 ± 0.3
J0613–0200 (b)	210.4°, –9.3°	3.061	480 ± 140	34.10	0.42	—	3.1 ± 0.7	3.1 ± 0.3	1.4 ± 0.2	2.9 ± 0.7	7 ± 4
J0751+1807 (b)	202.7°, 21.1°	3.479	620 ± 310	33.85	0.42	—	2.0 ± 0.7	1.7 ± 0.2	1.6 ± 0.2	3.4 ± 1.2	11 ± 11
J1614–2230 (b)	352.5°, 20.3°	3.151	1300 ± 250*	33.7	0.20	0.48	2.3 ± 2.1	2.5 ± 0.8	1.0 ± 0.3	1.2 ± 0.5	100 ± 80
J1744–1134	14.8°, 9.2°	4.075	470 ± 90	33.60	0.85	—	7.1 ± 1.4	4.0 ± 1.0	1.5 ± 0.2	1.1 ± 0.2	27 ± 12
J2124–3358	10.9°, –45.4°	4.931	250 ± 125	33.6	0.85	—	2.9 ± 0.5	3.4 ± 0.3	1.3 ± 0.2	2.9 ± 0.9	6 ± 6

[1]Space Science Division, Naval Research Laboratory, Washington, DC 20375, USA. [2]W. W. Hansen Experimental Physics Laboratory, Kavli Institute for Particle Astrophysics and Cosmology, Department of Physics, and SLAC National Accelerator Laboratory, Stanford University, Stanford, CA 94305, USA. [3]Santa Cruz Institute for Particle Physics, Department of Physics and Department of Astronomy and Astrophysics, University of California, Santa Cruz, CA 95064, USA. [4]Oskar Klein Centre for Cosmo Particle Physics, AlbaNova, SE-106 91 Stockholm, Sweden. [5]Department of Astronomy, Stockholm University, SE-106 91 Stockholm, Sweden. [6]Istituto Nazionale di Fisica Nucleare, Sezione di Pisa, I-56127 Pisa, Italy. [7]Laboratoire AIM, CEA/IRFU/CNRS/Université Paris Diderot, Service d'Astrophysique, CEA Saclay, 91191 Gif-sur-Yvette, France. [8]Istituto Nazionale di Fisica Nucleare, Sezione di Trieste, I-34127 Trieste, Italy. [9]Dipartimento di Fisica, Università di Trieste, I-34127 Trieste, Italy. [10]Department of Physics and Astronomy, Rice University, Houston, TX 77251, USA. [11]Istituto Nazionale di Fisica Nucleare, Sezione di Padova, I-35131 Padova, Italy. [12]Dipartimento di Fisica "G. Galilei," Università di Padova, I-35131 Padova, Italy. [13]Department of Physics, Center for Cosmology and Astroparticle Physics, Ohio State University, Columbus, OH 43210, USA. [14]Istituto Universitario di Studi Superiori, I-27100 Pavia, Italy. [15]Istituto Nazionale di Fisica Nucleare, Sezione di Perugia, I-06123 Perugia, Italy. [16]Dipartimento di Fisica, Università degli Studi di Perugia, I-06123 Perugia, Italy. [17]Dipartimento di Fisica "M. Merlin" dell'Università e del Politecnico di Bari, I-70126 Bari, Italy. [18]Istituto Nazionale di Fisica Nucleare, Sezione di Bari, I-70126 Bari, Italy. [19]Laboratoire Leprince-Ringuet, École Polytechnique, CNRS/IN2P3, Palaiseau, France. [20]Department of Physics, University of Washington, Seattle, WA 98195, USA. [21]Columbia Astrophysics Laboratory, Columbia University, New York, NY 10027, USA. [22]INAF–Istituto di Astrofisica Spaziale e Fisica Cosmica, I-20133 Milano, Italy. [23]Department of Physics, Royal Institute of Technology (KTH), AlbaNova, SE-106 91 Stockholm, Sweden. [24]NASA Goddard Space Flight Center, Greenbelt, MD 20771, USA. [25]George Mason University, Fairfax, VA 22030, USA. [26]Laboratoire de Physique et Chimie de l'Environnement, UMR 6115 CNRS, F45071 Orléans Cedex 02, and Station de Radioastronomie de Nançay, Observatoire de Paris, CNRS/INSU, F18330 Nançay, France. [27]Laboratoire de Physique Théorique et Astroparticules, Université Montpellier 2, CNRS/IN2P3, Montpellier, France. [28]Department of Physics and Astronomy, Sonoma State University, Rohnert Park, CA 94928, USA. [29]Department of Physics, Stockholm University, AlbaNova, SE-106 91 Stockholm, Sweden. [30]University of Maryland, Baltimore County, Baltimore, MD 21250, USA. [31]Agenzia Spaziale Italiana (ASI) Science Data Center, I-00044 Frascati (Roma), Italy. [32]Dipartimento di Fisica, Università di Udine and Istituto Nazionale di Fisica Nucleare, Sezione di Trieste, Gruppo Collegato di Udine, I-33100 Udine, Italy. [33]CNRS/IN2P3, Centre d'Études Nucléaires Bordeaux Gradignan, UMR 5797, 33175 Gradignan, France. [34]Université de Bordeaux, Centre d'Études Nucléaires Bordeaux Gradignan, UMR 5797, 33175 Gradignan, France. [35]Arecibo Observatory, Arecibo, PR 00612, USA. [36]Department of Physical Sciences, Hiroshima University, Higashi-Hiroshima, Hiroshima 739-8526, Japan. [37]University of Maryland, College Park, MD 20742, USA. [38]University of Alabama, Huntsville, AL 35899, USA. [39]Australia Telescope National Facility, Commonwealth Scientific and Industrial Research Organisation (CSIRO), Epping, NSW 1710, Australia. [40]Waseda University, 1104 Totsukamachi, Shinjukuku, Tokyo 1698050, Japan. [41]Cosmic Radiation Laboratory, Institute of Physical and Chemical Research (RIKEN), Wako, Saitama 3510198, Japan. [42]Department of Physics, Tokyo Institute of Technology, Meguro City, Tokyo 152-8551, Japan. [43]Centre d'Étude Spatiale des Rayonnements, CNRS/UPS, BP 44346, F-30128 Toulouse Cedex 4, France. [44]Jodrell Bank Centre for Astrophysics, School of Physics and Astronomy, University of Manchester, Manchester M13 9PL, UK. [45]Department of Physics, West Virginia University, Morgantown, WV 26506, USA. [46]Center for Research and Exploration in Space Science and Technology, NASA Goddard Space Flight Center, Greenbelt, MD 20771, USA. [47]Istituto Nazionale di Fisica Nucleare, Sezione di Roma "Tor Vergata," I-00133 Roma, Italy. [48]Department of Physics and Astronomy, University of Denver, Denver, CO 80208, USA. [49]Max-Planck-Institut für Extraterrestrische Physik, 85748 Garching, Germany. [50]National Radio Astronomy Observatory (NRAO), Charlottesville, VA 22903, USA. [51]Sterrenkundig Institut "Anton Pannekoek," 1098 SJ Amsterdam, Netherlands. [52]Institut de Ciencies de l'Espai (IEECCSIC), Campus UAB, 08193 Barcelona, Spain. [53]Institut für Astro- und Teilchenphysik, Leopold-Franzens-Universität Innsbruck, A6020 Innsbruck, Austria. [54]Space Sciences Division, NASA Ames Research Center, Moffett Field, CA 94035, USA. [55]NYCB RealTime Computing Inc., Lattingtown, NY 11560, USA. [56]Dipartimento di Fisica, Università di Roma "Tor Vergata," I-00133 Roma, Italy. [57]Department of Chemistry and Physics, Purdue University Calumet, Hammond, IN 46323, USA. [58]Institució Catalana de Recerca i Estudis Avançats, Barcelona, Spain. [59]Consorzio Interuniversitario per la Fisica Spaziale, I-10133 Torino, Italy. [60]Unit for Space Physics, NorthWest University, Potchefstroom Campus, Private Bag X6001, Potchefstroom 2520, South Africa. [61]School of Pure and Applied Natural Sciences, University of Kalmar, SE-391 82 Kalmar, Sweden.

*National Research Council Research Associate.
†Royal Swedish Academy of Sciences Research Fellow, funded by a grant from the K. A. Wallenberg Foundation.
‡To whom correspondence should be addressed. E-mail: guillemo@cenbg.in2p3.fr (L.G.); tyrel.j.johnson@nasa.gov (T.J.J.); kerrm@u.washington.edu (M.K.); smith@cenbg.in2p3.fr (D.A.S.)

temporaneous radio ephemerides with weighted root mean square timing residuals of 10 μs or less. For all eight MSPs, uncertainties in the dispersion measure led to uncertainties of less than 0.005 rotations in the extrapolation of the radio pulse arrival times to infinite frequency; such values are negligible for the gamma-ray light curve bin widths imposed by the photon counts. Analyses for PSRs J0218+4232, J0613–0200, J1614–2230, J1744–1134, and J2124–3358 using ephemerides from different observatories confirmed the absolute phase alignment.

We also searched for steady point-source emission at the locations of the 72 field MSPs. For 13 locations, including those of the eight pulsed detections, emission exceeded the diffuse gamma-ray background by at least 5σ. For the five sources for which only steady emission was seen, the 95%

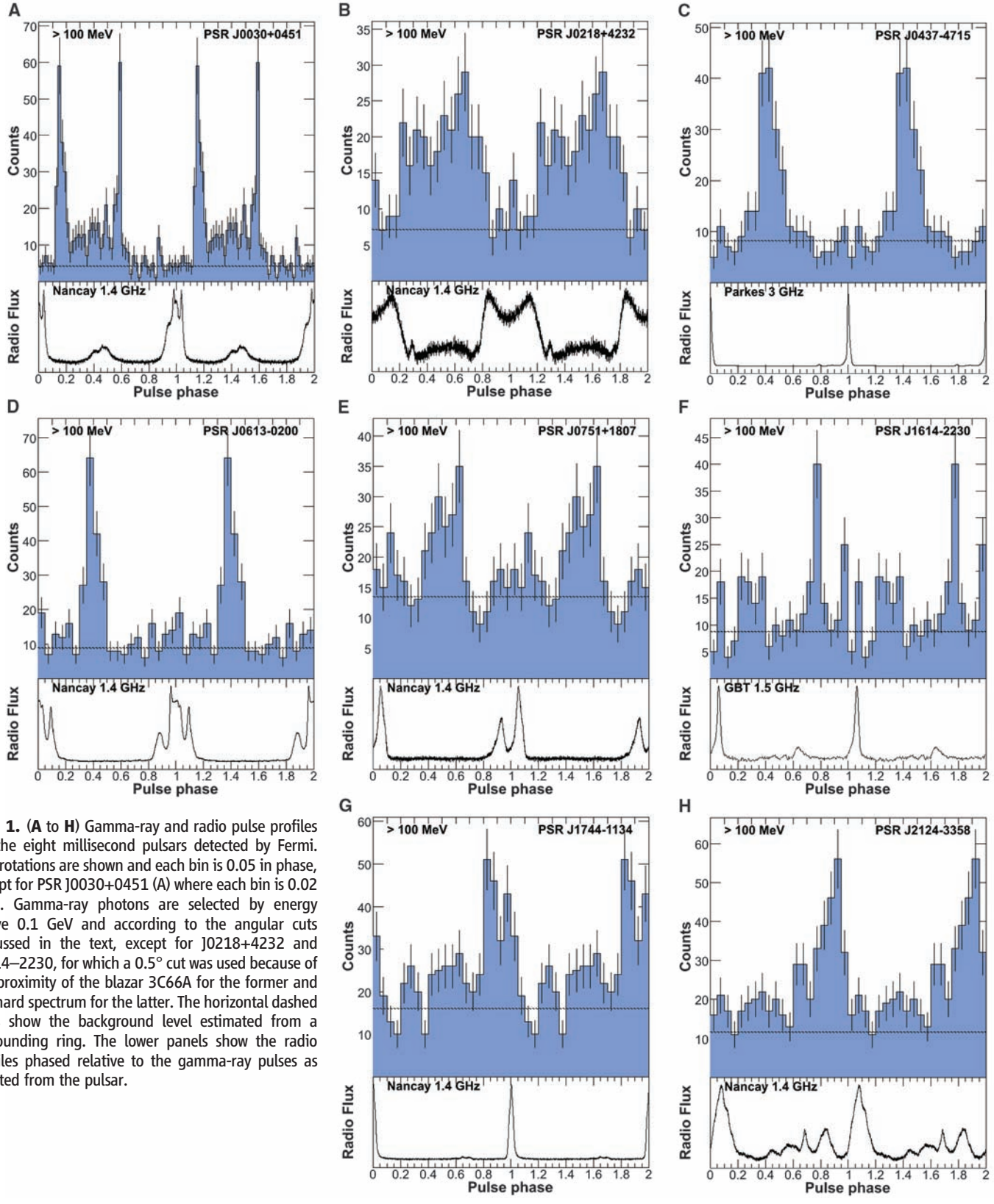

Fig. 1. (**A** to **H**) Gamma-ray and radio pulse profiles for the eight millisecond pulsars detected by Fermi. Two rotations are shown and each bin is 0.05 in phase, except for PSR J0030+0451 (A) where each bin is 0.02 wide. Gamma-ray photons are selected by energy above 0.1 GeV and according to the angular cuts discussed in the text, except for J0218+4232 and J1614–2230, for which a 0.5° cut was used because of the proximity of the blazar 3C66A for the former and the hard spectrum for the latter. The horizontal dashed lines show the background level estimated from a surrounding ring. The lower panels show the radio profiles phased relative to the gamma-ray pulses as emitted from the pulsar.

confidence level radii contained no other candidates besides PSRs J0034–0534, J0610–2100, J1600–3053, J1939+2134, and J1959+2048.

We used the spectral likelihood methods described in (*30*) (see supporting online text). To reduce the background from cosmic-ray interactions in the upper atmosphere, we required photon zenith angles to be less than 105° and excluded time periods when Earth's limb came within 28° of the source. Because of uncertainties in the instrument response, we rejected events with energies below 0.2 GeV. We modeled the gamma-ray spectra with an exponentially cut-off power law of the form $N_0 E^{-\Gamma} \exp[-(E/E_c)]$, where E is the photon energy, E_c is the exponential cutoff energy, Γ is the spectral index, and N_0 is a normalization factor (Table 1). The cutoff energies ranged from 1 GeV to almost 4 GeV (neglecting the J0218+4232 cutoff, which has a large error) and the spectra were hard ($\Gamma < 2$). Overall, the MSP spectral shapes resembled those of young pulsars.

We converted the integral energy fluxes h to luminosities using $L_\gamma = 4\pi h d^2$, where d is the pulsar distance. This corresponds to a flux correction factor $f_\Omega = 1$, appropriate for a fan-like beam as given by outer-magnetosphere emission models (*31*). Six of the pulsars are close and have parallax distance measurements (*32*–*34*), although uncertainties are large in some cases. The distances to PSR J0218+4232 and PSR J1614–2230 are based on the dispersion measures and the NE2001 galactic electron density model (*35*). MSPs have low intrinsic $\dot{P}$ values and are relatively close; hence, the kinematic Shklovskii contribution (*36*) $\dot{P}_s = P\mu^2 d/c$ (where μ is the proper motion) is non-negligible. $\dot{P}_s$ is subtracted from the observed $\dot{P}$ before computing the spin-down power $\dot{E}$ and the corresponding gamma-ray efficiency $\eta = L\gamma/\dot{E}$ (Table 1). Uncertainties in $\dot{E}$ are generally a few percent or less, except for PSRs J1614–2230 and J2124–3358, where they are larger (60% and 32%, respectively) because the large uncertainty in the distance leads to a correspondingly large uncertainty in $\dot{P}_s$. Uncertainties in η are much larger because $L_\gamma \sim d^2$ and hence the effect of the distance uncertainty is doubled. Such a large efficiency for PSR J1614–2230 would indicate that the distance is overestimated. Reducing the distance would both reduce the Shklovskii correction (thereby increasing $\dot{E}$) and decrease L_γ. Other possible systematic uncertainties in the $\dot{E}$ and η values come from the neutron star moment of inertia, which is assumed to be 10^{45} g·cm^2. Measured values of neutron star masses cover a range from about 1.25 to 1.75 solar masses (*37*, *38*), and the estimated moments of inertia vary correspondingly (*39*). Also, the flux correction factor f_Ω may differ from the assumed value of 1 (*31*).

Five of the eight gamma-ray MSPs are in binary systems. An eclipsing orbit, or interactions with the stellar wind of the companion, could affect the gamma-ray flux. We found no flux variability at their orbital periods (<25% of the flux at the 95% confidence level).

The observed MSP gamma-ray profiles and their relation to the radio profiles are similar to those observed for young pulsars. For PSRs J0030+0451 and J1614–2230, the double-peaked profiles with separation $\Delta \sim 0.45$ and first-peak lag $\delta \sim 0.15$ are almost identical to observed profiles for most young pulsars (*5*–*7*, *30*). A higher proportion of MSPs have a dominant single gamma-ray peak at $\delta \sim 0.5$, but the young pulsar PSR J2229+6114 has a similar pulse profile. For both MSPs and young pulsars, the gamma-ray peaks (single or multiple) are centered on phases 0.3 to 0.4 relative to the radio peak. MSP radio profiles tend to be complex with many components, and in these cases it can be difficult to identify the relevant radio phase. Also, the statistics of the gamma-ray profiles are currently relatively poor.

The spin-down powers of all the detected millisecond and normal gamma-ray pulsars lie above a common threshold of ~5×10^{33} ergs s^{-1} kpc^{-2}, another similarity between these two classes (Fig. 2). Pulsars undetected in gamma rays of both classes lie above this threshold, possibly because (i) distance estimates may be in error for individual pulsars; (ii) the gamma-ray emission beam (or at least strong parts of it) may not sweep across Earth; or (iii) neutron star moments of inertia may be less than the assumed 10^{45} g·cm^2 for some pulsars, so that a given $\dot{P}$ corresponds to a smaller $\dot{E}$.

Polar cap MSP models, where the bulk of the emission originates near the surface of the neutron star, predict that the pulsed gamma rays are roughly aligned with the magnetic poles (*40*). In outer gap (OG) (*41*) and slot gap (SG) (*42*) models, the bulk of the emission originates in the outer magnetosphere in narrow gaps along the last open field lines, forming wide fan beams that

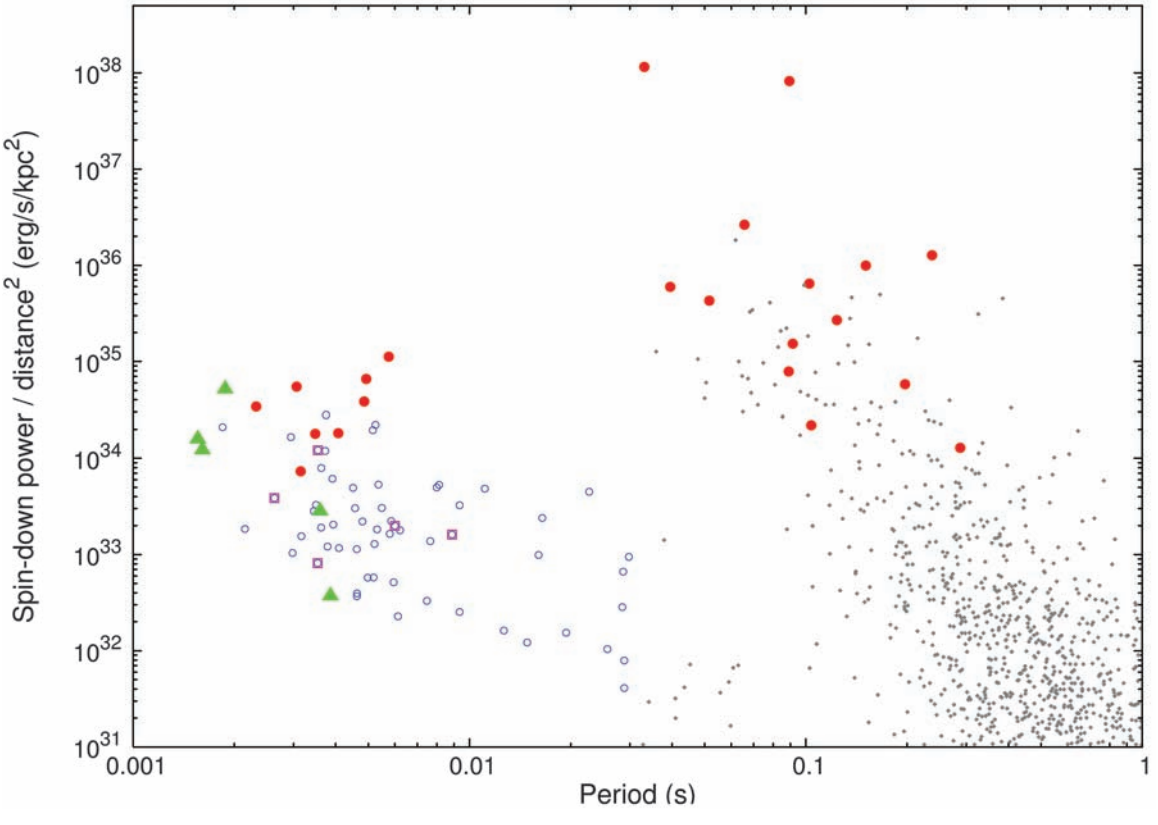

Fig. 2. Spin-down power $\dot{E}$ normalized to the distance squared versus the rotational period for pulsars outside of globular clusters. Where proper motions are available, the $\dot{E}$ values have been corrected for the Shklovskii effect (see text). The eight MSPs reported here are indicated by solid circles, as are young, radio-loud gamma-ray pulsars. The five MSPs likely associated with the nonpulsed point-source detections are indicated by triangles. MSPs for which contemporaneous rotation parameters are unavailable are shown as squares. Undetected MSPs are indicated by open circles, and small dots show undetected normal pulsars. The young radio-loud gamma-ray pulsars are the seven CGRO detections (*9*) and recent Fermi detections (*7*, *44*).

are not aligned with the magnetic poles. In the MSP gamma-ray light curves in Fig. 1, we see that although some of the gamma-ray peaks are aligned with the radio peaks that are thought to be aligned with the magnetic poles, most are not. This favors the outer-magnetosphere model geometry.

The similarities of the gamma-ray pulse profiles, the $\dot{E}$ dependence, and the spectral properties strongly suggest that the same basic emission mechanism is operating in both classes. Magnetic field strengths at the neutron star surface, derived assuming dipole fields, differ by four orders of magnitude between MSPs and young pulsars. On the other hand, B_{LC} is comparable for both. Fermi data for young pulsars (*5*–*7*, *30*) favor outer-magnetosphere emission models over models where the emission comes from close to the polar cap.

The MSP models (*40*–*42*) assume curvature radiation from electrons whose energies arise from a balance between acceleration by the pulsar electric field and the curvature radiation loss in a dipole magnetic field. The cutoff energy thus directly measures the accelerating electric field. The observed values in the range 1 to 4 GeV indicate that the emission is not taking place near the surface—where the electric field is stronger and the cutoff energies for MSPs would reach 10 GeV and could exceed 50 GeV (*43*)—but at some altitude above the neutron star surface.

For current SG and OG models, only MSPs with the highest spin-down power have a high enough electric potential for electron-positron pair production. Most of the MSPs detected by Fermi are below this threshold. Thus, some revision of the outer-magnetosphere models is needed. Surface magnetic fields may be stronger than assumed, perhaps because of magnetic multipoles or more compact neutron stars. Alternatively, the magnetic field at the light cylinder may play a greater role in particle acceleration than has been assumed.

References and Notes

1. D. C. Backer, S. R. Kulkarni, C. Heiles, M. M. Davis, W. M. Goss, *Nature* **300**, 615 (1982).
2. L. Kuiper *et al.*, *Astron. Astrophys.* **359**, 615 (2000).
3. A. A. Abdo *et al.*, *Astrophys. J.* **699**, 1171 (2009).
4. A. A. Abdo *et al.*, *Science* **325**, 840 (2009); published online 2 July 2009 (10.1126/science.1175558).
5. A. A. Abdo *et al.*, Fermi LAT Collaboration, *Astrophys. J.* **695**, L72 (2009).
6. A. A. Abdo *et al.*, *Astrophys. J.* **700**, 1059 (2009).
7. A. A. Abdo *et al.*, *Astrophys. J.* **699**, L102 (2009).
8. A. Pellizzoni *et al.*, AGILE Collaboration, *Astrophys. J.* **695**, L115 (2009).
9. D. J. Thompson *et al.*, *Astrophys. J.* **516**, 297 (1999).
10. W. B. Atwood *et al.*, *Astrophys. J.* **697**, 1071 (2009).
11. M. A. Alpar, A. F. Cheng, M. A. Ruderman, J. Shaham, *Nature* **300**, 728 (1982).
12. A. M. Archibald *et al.*, *Science* **324**, 1411 (2009); published online 21 May 2009 (10.1126/science.1172740).
13. D. R. Lorimer, M. Kramer, *Handbook of Pulsar Astronomy* (Cambridge Univ. Press, Cambridge, 2004).
14. L. Zhang, J. Fang, S. B. Chen, *Astrophys. J.* **666**, 1165 (2007).
15. S. A. Story, P. L. Gonthier, A. K. Harding, *Astrophys. J.* **671**, 713 (2007).
16. R. N. Manchester, G. B. Hobbs, A. Teoh, M. Hobbs, *Astrophys. J.* **129**, 1993 (2005).
17. The ATNF Pulsar Catalogue is available at www.atnf.csiro.au/research/pulsar/psrcat.
18. F. Camilo, F. A. Rasio, *ASP Conf. Ser.* **328**, 147 (2005).
19. D. A. Smith *et al.*, *Astron. Astrophys.* **492**, 923 (2008).
20. G. Theureau *et al.*, *Astron. Astrophys.* **430**, 373 (2005).
21. R. N. Manchester, *AIP Conf. Ser.* **983**, 584 (2008).
22. D. L. Kaplan *et al.*, *Publ. Astron. Soc. Pac.* **117**, 643 (2005).
23. G. Hobbs, A. G. Lyne, M. Kramer, C. E. Martin, C. Jordan, *Mon. Not. R. Astron. Soc.* **353**, 1311 (2004).
24. A. Dowd, W. Sisk, J. Hagen, *ASP Conf. Ser.* **202**, 275 (2000).
25. J. L. L. Voûte *et al.*, *Astron. Astrophys.* **385**, 733 (2002).
26. Fermi Science Support Center (http://fermi.gsfc.nasa.gov/ssc).
27. Fermi LAT Collaboration, http://arxiv.org/abs/0904.2226 (2009).
28. O. C. de Jager, B. C. Raubenheimer, J. W. H. Swanepoel, *Astron. Astrophys.* **221**, 180 (1989).
29. F. Crawford *et al.*, *Astrophys. J.* **652**, 1499 (2006).
30. A. A. Abdo *et al.*, Fermi LAT Collaboration, *Astrophys. J.* **696**, 1084 (2009).
31. K. P. Watters, R. W. Romani, P. Weltevrede, S. Johnston, *Astrophys. J.* **695**, 1289 (2009).
32. A. N. Lommen *et al.*, *Astrophys. J.* **545**, 1007 (2000).
33. A. T. Deller, J. P. W. Verbiest, S. J. Tingay, M. Bailes, *Astrophys. J.* **685**, L67 (2008).
34. A. W. Hotan, M. Bailes, S. M. Ord, *Mon. Not. R. Astron. Soc.* **369**, 1502 (2006).
35. J. M. Cordes, T. J. W. Lazio, http://arxiv.org/abs/astro-ph/0207156 (2002).
36. I. S. Shklovskii, *Sov. Astron.* **13**, 562 (1970).
37. M. Kramer *et al.*, *Science* **314**, 97 (2006); published online 14 September 2006 (10.1126/science.1132305).
38. J. P. W. Verbiest *et al.*, *Astrophys. J.* **679**, 675 (2008).
39. J. M. Lattimer, M. Prakash, *Science* **304**, 536 (2004).
40. A. K. Harding, V. V. Usov, A. G. Muslimov, *Astrophys. J.* **622**, 531 (2005).
41. L. Zhang, K. S. Cheng, *Astron. Astrophys.* **398**, 639 (2003).
42. A. G. Muslimov, A. K. Harding, *Astrophys. J.* **617**, 471 (2004).
43. T. Bulik, B. Rudak, J. Dyks, *Mon. Not. R. Astron. Soc.* **317**, 97 (2000).
44. A. A. Abdo *et al.*, *Astrophys. J. Suppl. Ser.* **183**, 46 (2009).

45. The Fermi LAT Collaboration is supported by NASA and the U.S. Department of Energy; the Commissariat à l'Énergie Atomique/IRFU and CNRS/Institut National de Physique Nucleaire et de Physique des Particules (France); the Agenzia Spaziale Italiana and Istituto Nazionale di Fisica Nucleare (Italy); the Ministry of Education, Culture, Sports, Science and Technology, High Energy Accelerator Research Organization (KEK), and Japan Aerospace Exploration Agency (Japan); and the K. A. Wallenberg Foundation, Swedish Research Council, and National Space Board (Sweden). Additional analysis during the operations phase was provided by the Istituto Nazionale di Astrofisica (Italy). The Parkes telescope is funded by the Commonwealth Government and is managed by CSIRO. The GBT is operated by the NRAO, a facility of NSF operated under cooperative agreement by Associated Universities Inc. The Arecibo Observatory is part of the National Astronomy and Ionosphere Center, operated by Cornell University under a cooperative agreement with NSF. The Nançay Radio Telescope is operated by the Paris Observatory, associated with the CNRS. The Lovell Telescope is owned and operated by the University of Manchester with support from the UK Science and Technology Facilities Council. The Westerbork Synthesis Radio Telescope is operated by ASTRON in the Netherlands.

Supporting Online Material

www.sciencemag.org/cgi/content/full/1176113/DC1
SOM Text
References

11 May 2009; accepted 24 June 2009
Published online 2 July 2009;
10.1126/science.1176113
Include this information when citing this paper.

Impact of Anode Microstructure on Solid Oxide Fuel Cells

Toshio Suzuki,[1]* Zahir Hasan,[1] Yoshihiro Funahashi,[2] Toshiaki Yamaguchi,[1] Yoshinobu Fujishiro,[1] Masanobu Awano[1]

We report a correlation between the microstructure of the anode electrode of a solid oxide fuel cell (SOFC) and its electrochemical performance for a tubular design. It was shown that the electrochemical performance of the cell was extensively improved when the size of constituent particles was reduced so as to yield a highly porous microstructure. The SOFC had a power density of greater than 1 watt per square centimeter at an operating temperature as low as 600°C with a conventional zirconia-based electrolyte, a nickel cermet anode, and a lanthanum ferrite perovskite cathode material. The effect of the hydrogen fuel flow rate (linear velocity) was also examined for the optimization of operating conditions. Higher linear fuel velocity led to better cell performance for the cell with higher anode porosity. A zirconia-based cell could be used for a low-temperature SOFC system under 600°C just by optimizing the microstructure of the anode electrode and operating conditions.

Although solid oxide fuel cells (SOFCs) are available commercially for local and emergency power generation, there are materials challenges that must be overcome for their wider use (*1*–*5*). Some of the features that make them attractive—their high efficiency and use with hydrocarbon fuels—stems from their high operating temperatures (often in excess of 700°C). These high temperatures are also a drawback in that transition metals used in the electrode materials can diffuse into the electrolyte and lower performance and, ultimately, lifetime. Thus, lowering the operation temperature can be beneficial for the commercialization of SOFC systems, since it can offer quick start-up ability, which in turn can allow for their use in applications such as transportable power sources and auxiliary power units for automobiles. Many studies of SOFCs aim at lowering their operating temperature (*6*–*13*). In recent years, much effort has been devoted to the development of SOFCs, especially in the search for new electrode and electrolyte materials. Lanthanum gallate perovskite [e.g., (La, Sr)(Ga, Mg)O_3, or LSGM] is one of the successful materials for a low- or intermediate-temperature SOFC elec-

[1]Advanced Manufacturing Research Institute, National Institute of Advanced Industrial Science and Technology, Nagoya, 463-8560 Japan. [2]Fine Ceramics Research Association, Nagoya, 463-8560 Japan.

*To whom correspondence should be addressed. E-mail: toshio.suzuki@aist.go.jp